Revue Roumaine de Chimie, **2007**, *52*(3), 275–281

TEMPERATURE DEPENDENCE OF THE ALKYL CHAIN ORDERING IN TWO LYOTROPIC SYSTEMS

Maria Nicoleta GRECU,[a] Gabriela BURDUCEA,[b] Voicu GRECU,[c]
Rodica MOLDOVAN,[d*] Traian BEICA[a] and Irina ZGURA[a]

[a] National Institute of Materials Physics P.O.Box Mg- 07, Bucureşti-Măgurele R-077125, Roumania
[b]University „Titu Maiorescu", Bucharest Str. Dionisie Lupu nr. 70, sector 1, Bucharest, Roumania
[c]Faculty of Physics, University of Bucharest P.O,Box Mg- 11, Bucureşti-Măgurele R-077125, Roumania
[d] Roumanian Academy Center for Advanced Studies in Physics Calea 13 Septembrie nr. 13, Bucharest, Roumania;
E-mail: rodi@ infim.ro

Received April 17, 2006

X-band ESR spectra of the calamitic and discotic lyotropic nematic phases in sodium dodecyl sulphate (SDS)/decanol/water system, doped with paramagnetic nitroxide free radicals are analyzed in this paper. The studied temperature range was chosen to include phase transitions of the lyotropic systems. The variation of the surfactant hydrocarbon chains ordering versus temperature is determined by the hyperfine splitting tensor ($\underline{A}$) and the spectroscopic splitting tensor ($\underline{g}$) anisotropies. The temperature dependence of the molecular order parameters for both lyotropic systems and the corresponding angular fluctuations are presented and discussed.

INTRODUCTION

Surfactant micellar organization. Ionic surfactants are amphiphilic molecules that present a polar head and a hydrophobic tail. In the presence of an appropriate solvent, under certain temperature/concentration conditions, they have the capacity to form a large variety of micellar shapes and structures as a result of a complex process of aggregation. In these conditions they are considered to be "lyotropic liquid crystals". Micellar structures, also called "phases", have been studied by X-Ray and neutron scattering and by NMR techniques that revealed the existence of the main types: lamellar, cubic, hexagonal and nematic.[1]

The nematic phase of the lyotropic liquid crystals occurs in ternary solutions when adding a long chain alcohol in the ionic surfactant aqueous solution if the amphiphilic molecule has the polar head of the sulphate, carboxylate, or alkyl ammonium type and the tail of linear hydrocarbon type with more than 8 carbon atoms, or if it is a fluorocarbon short chain derivative.[1-3] The nematic structures generally have a rather narrow temperature/concentration domain of existence.[4] The $\overline{n}$ director that defines the mean orientation of the micelles in the nematic phase is chosen to describe the mean orientation of the l_y axis for a calamitic micelle and that of the l_z axis for a discotic micelle. The common shape of the nematic micelle can be described as an ellipsoid with three distinct axes: l_x, l_y, l_z.[5] The $l_y >> l_x \cong l_z$ situation corresponds to the calamitic micelles (N_c phase) and the $l_z << l_x \cong l_y$ situation corresponds to the discotic micelles (N_d phase).

In this paper, we present the temperature dependence of the orientation degree of the amphiphilic molecules in the micelles of two nematic phases (N_c and N_d) of the lyotropic system SDS/water/decanol, determined by ESR spectroscopy studies. Liquid crystals do not generally have paramagnetic centers. ESR spectroscopy investigation supposes the insertion of that kind of centers, called "spin markers", conveniently chosen to reflect as close as possible the liquid crystal dynamics. The most appropriate

* Corresponding author.

spin markers to study lyotropic liquid crystals are fatty acids with a nitroxid radical group insertion (Fig. 1). This insertion can be made in different positions along the aliphatic chain. For example, the n-DX symbolizes the stearic acid marked with the doxyl group inserted strictly after the n^{th} carbon atom from the hydrophilic tail.

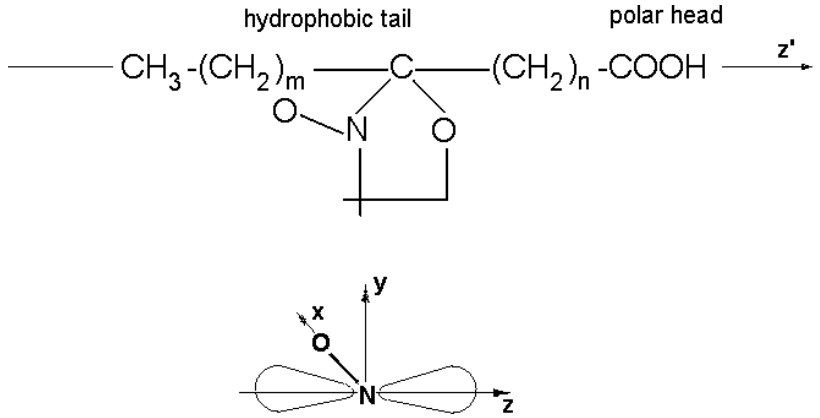

Fig. 1 – Spin marker I(*m,n*)- general structure (upward) and detail of the 2pπ orbital (downward); (*x,y,z*) is the rectangular coordinates system attached to the doxyl radical; *z'* is the long molecular axis direction of the surfactant molecule in the vicinity, initially supposed to be parallel to the *z* axis.

We denote by θ_i (i = 1, 2, 3), the angles between the three axes of a rectangular system attached to the marker molecule and the long axis *z'* of a surfactant molecule localized in the marker proximity, chosen as reference. The doxyl radical main directions are: the *x* axis corresponds to the N-O bond, *xy* being the doxyl ring plane; the *z* axis, perpendicular to the *xy* plane, corresponds to the unpaired nitrogen orbital $2p_z$ which is oriented along the fatty acid long axis (see Fig. 1). Then:

$$\cos\theta_1 = \vec{x}\cdot\vec{z}',\ \cos\theta_2 = \vec{y}\cdot\vec{z}',\ \cos\theta_3 = \vec{z}\cdot\vec{z}' \tag{1}$$

The diagonal components of the Seelig's order parameter tensor, $\underline{S}$ are expressed as the averages: [6]

$$S_{ii} = \frac{1}{2}\left\langle 3\cos^2\theta_i - 1\right\rangle \quad i = 1, 2, 3 \tag{2}$$

S_{11}, S_{22} and S_{33} are correlated to the mean angular fluctuations $\langle\theta_1\rangle$, $\langle\theta_2\rangle$, $\langle\theta_3\rangle$. Only two of the three order parameters are independent, as:

$$S_{11} + S_{22} + S_{33} = 0 \tag{3}$$

The microscopic order parameters S_{ii} are calculated using the ESR experimental data.

Analysis of ESR spectra for liquid crystalline states. The ESR spectrum of a free radical of that kind is described by a spin Hamiltonian:

$$\mathcal{H} = \beta\overline{B}\cdot\underline{g}\cdot\overline{S} + \overline{S}\cdot\underline{A}\cdot\overline{I} \tag{4}$$

where β is Bohr magneton, $\overline{S}$ is the electronic spin momentum and $\overline{I}$, the nuclear one. $\underline{g}$ and $\underline{A}$ are the tensors describing the anisotropic interaction with the magnetic field $\overline{B}$ and the hyperfine interaction with the nuclear spin of ^{14}N atom (I=1), respectively. In a rigid matrix (*e.g.* monocrystal, frozen state) the ESR spectrum is anisotropic and furnishes the values and the main directions of those tensors. For 5-DX marker used in experiments, g_x=2.0089, g_y=2.0062, g_z=2.0027 and A_x=6.4G, A_y=5.9G, A_z=33.5G.[7]

To find the $\underline{g}$ and $\underline{A}$ tensors compounds in the laboratory system, the self-system coordinates must be transformed into the laboratory system coordinates. In the laboratory reference system, the spin Hamiltonian becomes:

$$\mathcal{H} = \beta\bar{B} \cdot \underline{g}^{(L)}_{(t)} \cdot \bar{S} + \bar{S} \cdot \underline{A}^{(L)}_{(t)} \cdot \bar{I} \tag{5}$$

$\underline{A}^{(L)}_{(t)}$ and $\underline{g}^{(L)}_{(t)}$ tensors depend on the nitroxide free radical orientation in the above mentioned co-ordinate system. In their turn, these orientations are dependent of time and of molecular dynamics. There are no easy solutions to solve the dynamic problem. Approximations depending on the ratio between the calamitic dynamic correlation time $\tau_{\|}$ and the ESR spectroscopic characteristic measure time $\tau_{char} \approx 10^{-9}$ - 10^{-10} s, can be developed. The most frequently used approximation is that of rapid molecular movement $\tau_{\|} << \tau_{char}$ [8]. In this case, the rapid molecular movements partially mediate the orientation parameters and the spin Hamiltonian expression contains the mediated values:

$$\mathcal{H} = \beta\bar{B} \cdot \left\langle \underline{g}^{(L)}_{(t)} \right\rangle \cdot \bar{S} + \bar{S} \cdot \left\langle \underline{A}^{(L)}_{(t)} \right\rangle \cdot \bar{I} \tag{6}$$

So, the dynamic problem turns into a static one with values depending on mediation effects. We considered as rapid molecular movements the following ones: the rapid rotation of the n-DX molecule around its long axis (both $\underline{g}$ and $\underline{A}$ tensors are axial in the (x', y', z') reference system); the rapid diffusion in the micellar surface and the rapid rotation around the $\bar{n}$ micellar director (that coincides to the micellar rotation symmetry axis).

Due to physical considerations generated by the micellar dimensions, their dynamics towards the nematic phase $\bar{n}$ director cannot longer be treated in this approximation. Because of the axial symmetry of the molecular dynamics, the mediated tensors $\left\langle \underline{g}^{(L)}_{(t)} \right\rangle$ and $\left\langle \underline{A}^{(L)}_{(t)} \right\rangle$ have an axial symmetry and represent parameters that can be correlated to the ESR spectra shape in both nematic and isotropic phases. The molecular order parameters are expressed as:[6]

$$S_{33} = a(A_{\|} - A_{\perp}) / a'(A_{zz} - A_{xx}) \tag{7}$$

$$S_{11} = [3(g_{\|} - g_{iso}) - 2S_{33}(g_{zz} - g_{yy})] / 2(g_{xx} - g_{yy}) \tag{8}$$

where:

$$a = \frac{1}{3}(A_{xx} + A_{yy} + A_{zz}); \quad a' = \frac{1}{3}(A_{\|} + 2A_{\perp});$$

$$g_{iso} = \frac{1}{3}(g_{xx} + g_{yy} + g_{zz})$$

are isotropic parameters describing the spectrum in an isotropic medium characterized by rapid motion. Such a spectrum is a hyperfine triplet with equidistant resonance lines and intensities that can be different on account of the line width difference. The relaxation theory in isotropic liquids correlates these widths to a rotational relaxation time.

The paper is organized as follows: In the introductive chapter, essential information about the domain of the nematic liquid crystals are given and mostly of the topics in correlation with this paper interest such as physical and chemical considerations about the nematic phase, are developed. Mathematical support to understand the theory of analyzing ESR spectra applied to nematics is also given. Then, in the experimental chapter, it is presented the preparation procedure to obtain the lyotropic ternary solutions of the ionic surfactant, sodium dodecyl sulphate (SDS)/decanol/water in the calamitic phase (N_c) and the discotic phase (N_d.). The spin marker doping process is also described together with the ESR experimental measurements peculiarities. Finally, the ESR spectra shape changes with

temperature, including phase transitions, for both nematic lyotropic systems in the study are discussed, as well as the fluctuations with temperature of the three order parameters. The paper ends with some conclusions on the experimental work.

EXPERIMENTAL PART

Materials and sample preparation. To obtain lyotropic solutions we used SDS (Sigma, 99 % purity) without further purification, 1-decanol (Merck, 99 % purity) and triply distillated water. The used method was previously described.[9]

The compositions (wt %) of the two studied solutions, chosen from the phase diagram known in literature[10] in order to obtain nematic calamitic (N_c) and nematic discotic (N_d) liquid crystals at room temperature, were as follows:

N_c: 25.05(SDS) / 4.48(decanol) / 70.46(water)

N_d: 22.38(SDS) / 4.90(decanol) / 72.72(water)

For the investigation by ESR spectroscopy we used the spin marker 5-doxyl-stearic acid (5-DX) with the molar weight M=385 Kg/Kmol (Aldrich). It belongs to the so-called I(m,n) type with n=5 and is a (n + 2) doxyl derivative of the (m + n + 3)-carbon fatty acids family, with the general structure shown in Fig. 1.

The doping used (mol 5-DX/mol SDS) was 5-DX/$N_c \approx$ 1/700 and 5-DX/$N_d \approx$ 1/500. At these concentrations, the spin marker solubility was very good. When choosing the quantity of 5-DX, we had in view to minimize the spin-spin interactions in order to increase the spin-lattice interactions effect.[11,12] The high polarity of the N_d solution was also considered.

To homogenize solutions we applied both slow rotation (2 rot/min for 48 h) and ultrasonic procedures to the vessel in order to avoid the foaming of the lyotropic solutions. After preparation, we kept the samples into a thermostatted space at 23(±1)°C, to avoid degradation.

Transition temperatures for both lyotropic systems were measured directly, using the polarizing microscopy, as previously described.[13] We found that the nematic-isotropic phase transition took place at 29.7°C for the N_c sample and at 28.6°C for the N_d sample. We also found that for the N_d sample, after 30°C, the isotropic phase turned into a new anisotropic phase with a birefringent texture, probably a lamellar one.[14]

ESR measurements. To measure the ESR spectra of the nematic samples we used a JEOL spectrometer JES-ME-3 type in X-band (9.45GHz) on-line with a PC. To calibrate the magnetic field we used a MgO:Mn^{2+} standard probe. The nematic liquid crystal was sucked into capillary tubes (150 Kapilar Euroglass) at the room temperature. During the filling process, the calamitic micelles of the N_c probe orient in average with their long l_y axis parallel to the tube axis, while discotic micelles of the N_d probe orient in average with their short l_z axis perpendicular to the tube axis. During the recording of ESR spectra, the direction of the external magnetic field was perpendicular to the tube axis. ESR spectra were recorded between the 3rd and the 4th line of the manganese standard, while the external magnetic field was varied between 3200-3300G. The microwave field frequency was measured with a digital Takeda Riken 5502D. The temperature was measured with ±0.5°C precision. After modifying the temperature, we waited about 30 min. in order to reach the thermal equilibrium.

RESULTS AND DISCUSSION

As an example, the experimental ESR spectra of N_c solution are shown in Fig. 2. As a result of the ESR spectra analyses, we have obtained the experimental values in Table 1 and Table 2.

The ESR parameters analysis leads to the following observations. For the N_c sample, above the transition temperature, *a'* values decrease with a unit, indicating a decreasing polar influence in the marker vicinity. That happens only if micelle curvature modifies, so we conclude that the micellar axial ratio must decrease at the transition temperature. NMR measurements on samples having about the same composition[10] show the same phenomenon. For the N_d sample, *a'* values continue to increase above transition temperature. This remark is in complete agreement with NMR results on similar samples that indicate an increasing axial micellar ratio after transition.

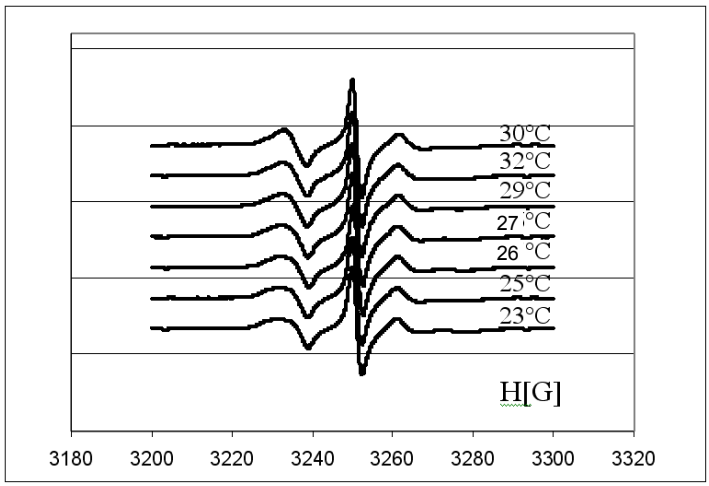

Fig. 2 – ESR spectra for the N_c sample.

The $g_{\|}$ values are lower for the N_c sample than for the N_d sample in the nematic domain and have an equalizing tendency after transition. On the other hand, we observed that $g_{\|} \neq g_{\perp}$ for each sample over all the tested temperature range, meaning that the paramagnetic centers have not an isotropic distribution in the post-transition domain. Quist[15] studied a N_c phase having a composition similar to ours and find out that it passes by a biphasic domain in a narrow temperature range (29÷32)°C before reaching the isotropic phase, instead of passing to the isotropic phase directly as the optical measurements show.[16] Our ESR results regarding the N_c solution seem to be in contradiction with the results of birefringence, which disappears at 29.7°C. To explain this we have to take into consideration that ESR spectroscopy gives information about the molecular local dynamics, while birefringence gives information about both molecular local dynamics in the micelle and micellar dynamics in the liquid crystal solution. For the N_d sample we found that our ESR experimental data, in agreement with the NMR results,[14] indicates that the N_d sample passes by a polyphase domain over 30°C, which is confirmed by optical measurements too.

Table 1

The experimental values of the ESR parameters for the N_c sample

T(°C)	$A_{\|}$ (G)	$A_{\perp}$ (G)	$g_{\|}$	$g_{\perp}$	a'
23	22.10	11.19	2.0042	2.0067	14.83
25	22.64	11.54	2.0041	2.0065	15.24
26	20.52	11.10	2.0053	2.0067	14.23
27	19.30	11.49	2.0057	2.0064	14.09
29	21.70	11.44	2.0041	2.0066	14.86
30	17.75	11.29	2.0055	2.0066	13.37
32	17.75	11.44	2.0057	2.0067	13.54

Table 2

The experimental values of the ESR parameters for the N_d sample

T(°C)	$A_{\|}$ (G)	$A_{\perp}$ (G)	$g_{\|}$	$g_{\perp}$	a'
24	17.30	11.14	2.0058	2.0069	13.19
25	16.86	11.14	2.0058	2.0067	13.05
26	16.86	11.14	2.0058	2.0066	13.05
30	17.74	11.43	2.0058	2.0066	13.53
33	18.30	11.63	2.0055	2.0066	13.85
35	18.29	11.73	2.0055	2.0066	13.92

The values of the dynamic parameters for the nematic calamitic N_c and the nematic discotic N_d solutions, calculated by applying Eqs. (2), (5), (9) and (10), are synthesized in Table 3.

The order parameters values evaluation leads to the following observations. At temperatures in the nematic phase (T<29.8° for N_c and T<29.5°C for N_d phase, as it results from the fit of the data in Fig. 3), S_{33} order parameter values for the N_c phase are about twice higher than those for the N_d phase, reflecting that the hydrocarbon chains are more confined in the calamitic micelle than in the discotic micelle. We explain that by the fact that the spin marker, which generally locates in the micellar minima curvature zone,[17] is located in a lower curvature zone in the discotic micelle than in the calamitic micelle.

Table 3

The microscopic order parameters values for the N_c and N_d samples

T°C	S_{33}		$\bar{\theta}_3$ (deg)		S_{11}		$\bar{\theta}_1$ (deg)		S_{22}		$\bar{\theta}_2$ (deg)	
	N_c	N_d	N_c	N_d	N_c	N_d	N_c	N_d	N_c	N_d	N_c	N_d
23	0.42	-	38	-	-0.40	-	75	-	-0.02	-	55	-
24	-	0.24	-	45	-	0.24	-	45	-	-0.49	-	90
25	0.41	0.24	39	45	-0.46	0.24	80	45	0.05	-0.48	53	89
26	0.37	0.24	40	45	0.12	0.24	50	45	-0.49	-0.48	85	89

Table 3 (continues)

Table 3 (continued)

29	0.39	-	40	-	-0.49	-	85	-	0.10	-	60	-
30	0.27	0.26	45	45	0.10	0.24	51	45	-0.37	-0.50	73	90
32	0.26	-	45	-	0.20	-	47	-	0.46	-	81	-
33	-	0.27	-	45	-	0.10	-	51	-	-0.37	-	73
35	-	0.26	-	45	-	0.09	-	51	-	-0.35	-	72

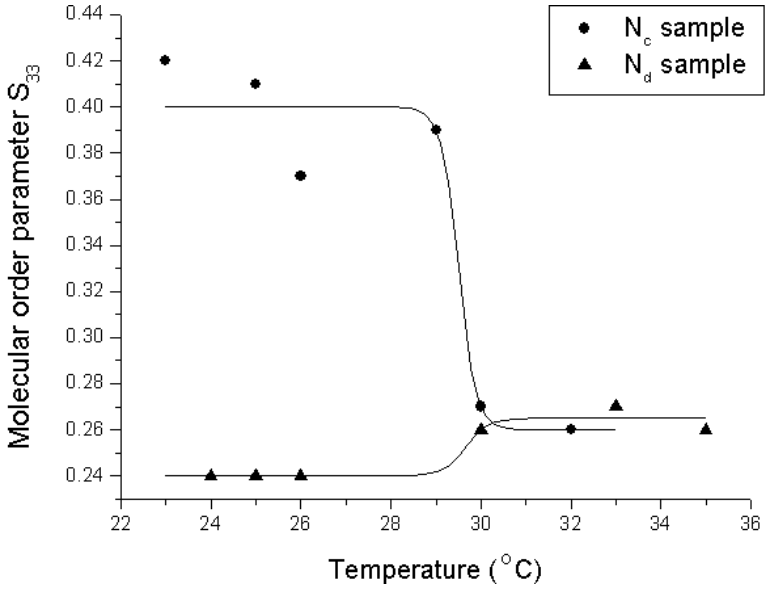

Fig. 3 – Temperature dependence of the molecular order parameter S_{33} for the liquid crystal samples. The continue line is the fit with the sigmoidal function: $S_{33} = A_2 + (A_1 - A_2)/\{1 + \exp[(T - T_0)/dx]\}$.
●- experimental results for the N_c sample; fit parameters A_1=0.24; A_2=0.26; T_0=29.8; dx=0.146;
▲- experimental results for the N_d sample; A_1=0.4; A_2=0.26; T_0=29.5; dx=0.195.

In Fig. 3 we remark the nematic – isotropic transition for the N_c sample by the abruptly reducing of the S_{33} order parameter value at 29.8°C, in accordance with the optical study. The corresponding average angular fluctuations are increasing slowly and continuously. Increasing disorder at the hydrocarbon tales level can be explained by changes in their packing shape. The lower S_{33} value after transition confirms the conclusion that micellar axial ratio decreases after transition. The two other parameters, S_{11} and S_{22} have disparate positive and negative values, while the corresponding average angular fluctuations values (bigger than 50º) show that *x* and *y* axes of the spin marker molecule are significantly inclined towards the *z'* axis.

For the N_d sample, as we can see from Tab. 3 and Fig. 3, the S_{33} order parameter is constant with temperature in the nematic phase and shows only a slight increase after transition. After transition, both S_{33} and S_{11} parameters have low values, close to the N_c sample values. The S_{22} parameter has rather high negative values in the nematic domain and decreases after transition. Because of the slight increase of the S_{33} order parameter values after transition at about 30°C, we have concluded that for the N_d sample, a bilayer-like structure continues to exist, probably lamellar fragments or discotic micelles of different dimensions than the micelles in the N_d phase. This conclusion is also concordant with NMR investigation.[14]

CONCLUSIONS

The ESR spectroscopy technique to investigate local molecular ordering degree for the lyotropic ternary system sodium dodecyl sulphate/ decanol/ water in the nematic calamitic and discotic phases was able to evidence the nematic to isotropic phase transition. From the final ESR parameters comparative analysis data we formulate the following remarks:

For the N_c solution the micellar axial ratio decreases after transition, while for the N_d solution it increases after transition, in concordance with

NMR investigations[14,15] for nematics with compositions close to ours;

For both solutions, the post-transition domain is not an isotropic one from the paramagnetic centers distribution point of view, in agreement with NMR studies[14,15];

In the nematic phase, S_{33} order parameter values for the N_c phase are about twice higher than those for the N_d phase, reflecting that the hydrocarbon chains are more confined in the calamitic micelle than in the discotic micelle.

The totality of the average angular fluctuations values demonstrates that the ionic surfactant hydrocarbon chain dynamics for both N_c and N_d solutions are similar and are generated by small angle torsions and C-C bond flexions with activation probabilities and energies depending on pre- and post-transition thermodynamic conditions and on the samples structures. We must not minimize the fact that the spin marker molecule may have a slightly different behavior from the surfactant molecules in the vicinity, because of the larger space around its long chain axis. The ring at which N-O is attached is asymmetric and that asymmetry may be a reason for the nonlinearity of the fatty acid chain, probably also induced to the surfactant chains in the vicinity.

Experimental data demonstrate that modifications in the thermodynamic conditions generate a variation of the disorder at the level of the surfactant molecule hydrocarbon chain for both N_c and N_d solutions, but this is manifested in a different way.

Acknowledgements: Some of the authors (R.M., T.B., I.Z.) thank the Roumanian Ministry of Education and Research for financial support under the CEX Project D11-76.

REFERENCES

1. C. Fairhurst, S. Fuller, J. Gray, M. C. Holmes and G. J. T. Tiddy, in "Handbook of Liquid Crystals", D. Demus, J. Goodby, G. W. Gray, H-W. Spiess and V. Vill (Eds.), Willey-VCH, Weinheim, New York, 1998, vol. 3, p.341-392.
2. K. W. Lawson and T. J. Flaut, *J. Am. Chem. Soc*., **1967**, *89*, 5489-5491.
3. L. Q. Amaral and A. M. F. Neto, *Mol. Cryst. Liq. Cryst.*, **1983**, *98*, 285-290.
4. A. S. Sonin, *Usp. Fiz. Nauk*, **1987**, *153*, 274-310.
5. P. Toledano and A. M. F. Neto, V. Lorman, B. Mettout, V. Dmitriev, *Phys. Rev. E*, **1995**, *52*, 5040-5052.
6. J. Seelig, *J. Am. Chem. Soc.*, **1970**, *92***,** 3881-3887.
7. T. Risse, T. Hill and J. Schmidt, G. Abend, H. Hamann, H.-J. Freund, *J. Phys. Chem. B*, **1998**, *102*, 2668-2676.
8. P. V. Shui, G. B. Birrell and G. O'Hayes, *J. Magn. Res.*, **1974**, *15***,** 444-449.
9. T. Beica, R. Moldovan, M. R. Puica and S. Frunza, *Liq. Cryst.*, **2002**, *29*, 1275-1278.
10. P. O. Quist, B. Halle and I. Furo, *J. Chem. Phys.*, **1992**, *96*, 3875-3891.
11. A. Arcioni, C. Bacchiocchi, L. Grossi, A. Nicolini and C. Zannoni, *J. Phys. Chem. B*, **2002**, *106*, 9245-9252.
12. Z. Liang, G. Wikander and P-O. Westlund, *J. Chem. Phys.*, **1995**, *102*, 1471-1480.
13. T. Beica, R. Moldovan, M. Tintaru, M. R. Puica, I. Enache and S. Frunza, *Liq. Cryst.*, **2004**, *31*, 325-332.
14. I. Furo, B and Halle, *Phys.Rev. E*, **1995**, *51* , 466-476.
15. P. O. Quist and B. Halle, I. Furo, *J. Chem. Phys.* **1991,** *95*, 6945-6951.
16. T. Beica, R. Moldovan, M. Tintaru, I. Enache and S. Frunza, *Cryst. Res. Technol.* **2004**, *39*, 151-156.
17. Y. Hendrix, J. Charvolin and M. Rawiso, *J. Colloid Interface Sci.* **1984**, *100*, 597-601.